BNL-33483

Subm. to EPS International Europhysics Conf. on High Energy Physics, Brighton, UK, July 20-27, 1983

OG 735

CONF-830718-5

BNL--33483

DE83 017349

# A STUDY OF EXCLUSIVE CENTRAL HADRON PRODUCTION AT THE ISR AS A SEARCH FOR GLUONIUM STATES

The Axial Field Spectrometer Collaboration

T. Akesson[4], M.G. Albrow[10], S. Almehed[6], R. Batley[4], O. Benary[11], H. Bøggild[5], O. Botner[5], H. Breuker[4], H. Brody[7], V. Burkert[2], A.A. Carter[9], J.R. Carter[3], P.C. Cecil[3], S.U. Chung[1], W.E. Cleland[8], D. Cockerill[10], R. Carosi[4], S. Dagan[11], E. Dahl-Jensen[5], I. Dahl-Jensen[5], P. Dam[4], G. Damgaard[5], W.M. Evans[10], C.W. Fabjan[4], P. Frandsen[4], S. Frankel[7], W. Frati[7], M. Gibson[10], U. Goerlach[4], M.J. Goodrick[3], H. Gordon[1], K.H. Hansen[5], V. Hedberg[6], J. Hiddleston[10], H.J. Hilke[4], J. Hooper[5], G. Jarlskog[6], P. Jeffreys[4], G. Kesseler[4], T. Killian[1], R. Kroeger[8], K. Kulka[6], J.v.d. Lans[4], J. Lindsay[4], D. Lissauer[11], B. Lörstad[6], T. Ludlam[1], A. Markou[4], N.A. McCubbin[10], U. Mjörnmark[6], R. Møller[5], W. Molzon[7], B.S. Nielsen[4], A. Nilsson[6], L.H. Olsen[4], Y. Oren[11], T.W. Pritchard[9], L. Rosselet[4], E. Rosso[4], A. Rudge[4], R. Schindler[4], M. Sullivan[8], I. Stumer[1], J.A. Thompson[8], G. Thorstenson[6], E. Vella[7], D. Weygand[1], J. Williamson[10], W.J. Willis[4], M. Winik[1], W. Witzeling[4], C. Woody[1], W.A. Zajc[7]

1 Brookhaven National Laboratory, Upton, NY USA.
2 Physikalisches Institut, Universitat Bonn, BRD.
3 Cambridge University, Cambridge, UK.
4 CERN, Geneva, Switzerland.
5 Niels Bohr Institute, Copenhagen, Denmark.
6 University of Lund, Sweden.
7 University of Pennsylvania, Philadelphia, PA USA.
8 University of Pittsburgh, Pittsburgh, PA USA.
9 Queen Mary College, London, UK.
10 Rutherford Appleton Laboratory, Didcot, UK.
11 University of Tel Aviv, Israel.

Paper 291
B4,B5,E3/P10,P11

# A STUDY OF EXCLUSIVE CENTRAL HADRON PRODUCTION AT THE ISR AS A SEARCH FOR GLUONIUM STATES


The Axial Field Spectrometer Collaboration

T. Akesson[4], M.G. Albrow[10], S. Almehed[6], R.Batley[4], O. Benary[11], H. Bøggild[5], O. Botner[5], H. Breuker[4], H. Brody[7], V. Burkert[2], A.A. Carter[9], J.R. Carter[3], P.C. Cecil[3], S.U. Chung[1], W.E. Cleland[8], D. Cockerill[10], R. Carosi[4], S. Dagan[11], E. Dahl-Jensen[5], I. Dahl-Jensen[5], P. Dam[4], G. Damgaard[5], W.M. Evans[10], C.W. Fabjan[4], P. Frandsen[4], S. Frankel[7], W. Frati[7], M. Gibson[10], U. Goerlach[4], M.J. Goodrick[3], H. Gordon[1], K.H. Hansen[5], V. Hedberg[6], J. Hiddleston[10], H.J. Hilke[4], J. Hooper[5], G. Jarlskog[6], P. Jeffreys[4], G. Kesseler[4], T. Killian[1], R. Kroeger[8], K. Kulka[6], J. v.d. Lans[4], J. Lindsay[4], D. Lissauer[11], B. Lörstad[6], T. Ludlam[1], A. Markou[4], N.A. McCubbin[10], U. Mjörnmark[6], R. Møller[5], W. Molzon[7], B.S. Nielsen[4], A. Nilsson[6], L.H. Olsen[4], Y. Oren[11], T.W. Pritchard[9], L. Rosselet[4], E. Rosso[4], A. Rudge[4], R. Schindler[4], M. Sullivan[8], I. Stumer[1] J.A. Thompson[8], G. Thorstenson[6], E. Vella[7], D. Weygand[1], J. Williamson[10], W.J. Willis[4], M. Winik[1], W. Witzeling[4], C. Woody[1], W.A. Zajc[7].



## ABSTRACT

We present a preliminary report on a study of the exclusive reaction $pp \to pph^+h^-$ ($h = \pi,K,p$) at $\sqrt{s} = 63$ GeV and $\sqrt{s} = 45$ GeV, with $h^+$ and $h^-$ in the central region. This reaction has been suggested as a method of searching for gluonium states. The mass distributions in the $\pi^+\pi^-$ system appear to be identical at the two values of $\sqrt{s}$. They show a rapid order of magnitude decrease in cross-section at 1000 MeV/$c^2$ and 1500 MeV/$c^2$. Further structure is observed above 2000 MeV/$c^2$.



1 Brookhaven National Laboratory, Upton, N.Y., USA.
2 Physikalisches Institut, Universität Bonn, BRD.
3 Cambridge University, Cambridge, UK.
4 CERN, Geneva, Switzerland.
5 Niels Bohr Institute, Copenhagen, Denmark.
6 University of Lund, Sweden.
7 University of Pennsylvania, Philadelphia, P.A., USA.
8 University of Pittsburgh, Pittsburgh, P.A., USA.
9 Queen Mary College, London, UK.
10 Rutherford Appleton Laboratory, Didcot, UK.
11 University of Tel Aviv, Israel.



Submitted to: Int. Europhysics Conference on High Energy Physics, Brighton, July 1983

# I. INTRODUCTION

We are investigating the properties of the mesonic system M produced via the exclusive reaction pp → pMp, where the state M consists of two charged particles which are contained in the central region $y \leq 1$ and are fully measured. The two final state protons have almost the full c.m. momentum of the incident protons ($x_F \geq 0.95$) and are well isolated in rapidity from the central region ( $y_p \sim 4.0$). The state M must have Q=B=S=0. In the framework of Regge theory such events are produced by double pomeron exchange (DPE) [1] and the quantum numbers of M are further constrained to be I=0, G=+1, C=+1. There are also constraints on the $J^P$ of M; for example for a $\pi^+\pi^-$ or $K^+K^-$ state thus produced one expects $J^P = 0^+, 2^+, 4^+$ etc. Such a highly constrained system is of great interest for meson spectroscopy, especially in view of the importance of establishing the existence (or non-existence) of gluonium states (glueballs) [2] and the interpretation of the pomeron in QCD as multiple gluon exchange [3]. The possible value of this reaction in gluonium searches was first pointed out by Robson [4].

Earlier experiments at lower c.m. energies [5] did not isolate the DPE process ; for example the presence of a clear $\rho^0$ signal in the $\pi^+\pi^-$ channel (forbidden for DPE) demonstrated a strong contamination from non-pomeron exchange. However at the highest ISR energies experiments [6] have obtained a signal with all the expected characteristics of DPE, but they were hitherto limited in both statistics and mass resolution. A signal was observed at $M_{\pi\pi}$ around 1300 MeV/$c^2$, attributed to the f(1270), but no other significant structures were seen.

In this paper we present high statistics data with good mass resolution on the $\pi^+\pi^-$ (exclusive) final state, and limited data on the exclusive $K^+K^-$ and $p\bar{p}$ central states, at $\sqrt{s}$= 63 GeV. We also have some data at $\sqrt{s}$= 45 GeV, which are referred to only in section V, where the $\pi^+\pi^-$ mass spectrum is presented.

## II. APPARATUS

The Axial Field Spectrometer (AFS) [7] is used for measuring the central hadrons. Charged particles are measured with up to 42 space-points per track in the cylindrical central drift chamber covering over 85% of the azimuth $\phi$ in $40° < \theta < 140°$ with $dp/p \sim 2.5\%\ p(GeV/c)$. Particles can be identified as $\pi$, K or $p(\bar{p})$ over most of the relevant mass region from dE/dx measurements in the chamber. (A full-azimuth electromagnetic and hadronic calorimeter and two walls of NaI crystals can be used for detection of $\pi^0, \eta^0, K^0_L$ etc. but were not needed for the present study of charged particle events).

To provide a trigger for this reaction and to measure the trajectories of the forward protons we installed four small (5cm x 5cm transverse dimensions) track detectors above (UP) and below (DOWN) each downstream beam pipe at a distance $z \sim 9$m from the intersection, see Fig. 1. Each track detector consists of three drift chambers spaced over 1.1 m and two $\sim$ 3cm x 3cm scintillation counters at the front and back. The drift chambers [8] each have four horizontal sense wires, the vertical (y-direction) drift distance being measured with a precision of $\sigma \sim 120$ μm per wire. The wires are equipped with charge division read-out to give the horizontal (x-direction) position to $\sigma \sim 1.2$mm (the wires are 5cm long ; only the central 3cm are used). A final state proton passes through the ISR vacuum for $\sim$ 8m before emerging through a thin (0.2mm stainless steel) window in a circular-elliptical pipe transition. Multiple scattering and magnetic deflections are negligible, and we measure dy/dz and dx/dz with $\sigma \sim 10^{-4}$ and $\sim 3\times10^{-4}$ respectively. Each forward track detector covers $3 \lesssim \theta \lesssim 8$ mrad over $\sim 45°$ of azimuth $\phi$.

Most of the solid angle not covered by the central detector or the forward track detectors was covered by $\sim$ 100 scintillation counters. The OR of these counters was used as a veto in the trigger logic. The trigger required an AND of the following conditions :

(i) a coincidence between the two scintillators in both forward 'UP' arms or both forward 'DOWN' arms (thus ensuring no background from elastic scattering),

(ii) at least 2 elements of a 44-scintillator central cylindrical 'barrel' hodoscope to have hits,

(iii) no detected charged particles in the angular regions covered by the veto counters.

## III. DATA TAKING AND RECONSTRUCTION

At $\sqrt{s}$= 63 GeV we present data from $\sim$ 930,000 triggered events, corresponding to $\sim$ 200 hours of running with a typical luminosity $\sim 1.7 \times 10^{31} cm^{-2} sec^{-1}$. Events were rejected if a second interaction occurred within 100 ns of the triggered event, using timing information from all the scintillator elements. Remaining events were analysed using the standard AFS pattern-recognition and track-fitting programs. We then selected for further analysis those events with two and only two central tracks, each with $\geq$ 30 degrees of freedom, $\geq$ 15 z-measurements (from charge division), $dp/p < 0.1$ and fitting to a common vertex. 12% of the triggers remain. We then calculate $\Sigma p_y$ for the central hadron pair ($p_y$ is the vertical momentum component) and show its distribution in fig. 2a for the UP.UP and DOWN.DOWN triggers separately. Distinct peaks occur centred at -0.32 GeV/c (for UP.UP) and + 0.32 GeV/c (for DOWN.DOWN) demonstrating clearly the presence of exclusive events. [As dy/dz for each forward track is $(5.25 \pm 2.5) \times 10^{-3}$ their momenta must be $\sim 0.32$ GeV/c/$(2 \times 5.25 \times 10^{-3}) \sim 30$ GeV/c as expected]. Less than 10 % of the events have Q= ±2 for the central pair, and for these events the $\Sigma p_y$ distribution, shown as the shaded area in Fig. 2a, shows no momentum-balancing peak as expected for non-exclusive events. Only Q=0 central pairs are retained.

We then applied further quality cuts on the central tracks (vertex fit $\chi^2$ and track length) and required that the vertex be within the interaction diamond. Tracks were identified using the truncated mean of the dE/dx measurements after correcting for an observed run-to-run variation resulting from small fluctuations in the drift chamber gain. All tracks were assigned to one of five identification classes : unambiguous $\pi$, K or p($\bar{p}$), $\pi$/K ambiguous or $\pi$/K/p ambiguous. A track was then required in each of the two forward drift chamber telescopes and its direction cosines found ; for dy/dz only the information from the telescope itself was used, while for dx/dz the central vertex position was included in the fit. We then calculated the momenta of the forward protons, assuming an exclusive 4-prong event and using the $p_z$ and E constraints. For this calculation the incident momenta were corrected for momentum compaction(i.e. the correlation between momentum and position within the beam) from the vertex position. The distribution of $\Sigma p_y$ of the four final state particles is then found to be centred at zero with $\sigma$=35 MeV/c ; a cut is applied at $\pm$ 60 MeV/c. Finally we calculate the difference between $\Sigma p_x$ of the initial (IN) and final (OUT) states (in the ISR lab. frame, $\Sigma p_x$(IN) $\sim$ 8 GeV/c). This is shown on a logarithmic scale in Fig. 2b, and shows a sharp peak centred at zero. The background due to residual non-exclusive events is shown as a dashed line. A cut is applied at $\pm$ 150 MeV/c which then contains $\sim$ 5% residual background (either non-exclusive events or events where one of the four tracks was badly measured).

This final sample contains 34839 events. As the events are exclusive (apart from the 5% background) it is sufficient to identify one of the two central hadrons unambiguously and to require that the other be consistent with having the same identity. In fact only 0.3% of the events in this final sample have inconsistent identification (eg K with $\pi$, or K/$\pi$ with p etc). Only 269 events are classified as $K^+K^-$, requiring at least one K to be uniquely identified, and 19 as $p\bar{p}$. The vast majority of the events (98.9%) are either uniquely identified as, or consistent with being, $\pi^+\pi^-$ and we take them as such. (Note that the K/$\pi$ ratio in this sample is much less than that in typical hadronic collisions at this energy.)

For the $\pi\pi$ events the distribution of Feynman x for the protons ($x_F = p_L^*/p_{max}^*$) is shown in Fig. 3a on a logarithmic scale (2 entries per event, with no correction applied for the acceptance of the apparatus). The distribution peaks strongly above $x_F$=0.99, 99.5% of the events having $x_F$ > 0.95. The range in t is $0.015 < |t| < 0.045$ $(GeV/c)^2$. The observed distributions of the rapidity of the central pions, and of the central $\pi\pi$ pair, are shown in Fig. 3b. The acceptance of the central detector (with the track quality cuts we required) cuts off the $y_\pi$ distributions at $|y| = 1$.

## IV. MASS SPECTRA AT $\sqrt{s}$ = 63GeV

Fig. 4a shows the effective mass distribution of the $\pi^+\pi^-$ events in 25 MeV/$c^2$ bins. The distribution rises rapidly from threshold, peaks at ~500 MeV/$c^2$ and then fall surprisingly slowly (not as fast as $1/M^2$) to 950 MeV/$c^2$, with no clear enhancement at the $\rho^0$ mass. Absence of the $\rho^0$ signal is evidence that background from reggeon exchange is small. The distribution drops very rapidly between 950 MeV/$c^2$ and 1050 MeV/$c^2$, and then shows a broad enhancement centred at 1300 MeV/$c^2$. This higher mass region is better shown with the expanded vertical scale in Fig. 4b. One sees again a relatively rapid drop between 1400 and 1600 MeV/$c^2$ followed by a rather flat continuum. However the extension of the mass scale in Fig. 4c shows (now in 50 MeV/$c^2$ bins) that this continuum decreases again over a relatively narrow mass interval from 2300-2500 MeV/$c^2$. Near 3000 MeV/$c^2$ there are few events, and none above 3500 MeV/$c^2$, although the geometrical acceptance is still close to its maximum value at high mass. In order to present the full mass range together, the complete distribution is shown in Fig. 5 with a logarithmic scale.

The data of Figs. 4 and 5 are not corrected for acceptance as a function of mass. A straightforward Monte Carlo has been used to simulate the DPE process, generating $t_1$, $t_2$ of the final protons exponentially as exp $(-\alpha|t|)$ and the rapidity of the central system uniformly within the range -1 to +1. The results are insensitive to the precise value of exponential slope parameter; $\alpha = 6.5$ $(GeV/c)^2$ has been used. To simulate an s-wave decay of the central system the $\pi^+\pi^-$ were produced isotropically in their overall rest frame. Simple geometrical cuts were imposed on the tracks. The resulting acceptance versus mass is shown in Fig.6. It clearly cannot give rise to the observed structures. We have carefully investigated whether the existence of definite momentum ranges for the identification of different particles can give rise to such effects, and conclude that they cannot. The mass resolution is calculated to be $\sigma_M \sim 15$ MeV/$c^2$ at 1000 MeV/$c^2$ rising to $\sigma_M \sim 27$ MeV/$c^2$ at 2200 MeV/$c^2$. We estimate a possible systematic error on the mass scale of 20 MeV/$c^2$ at 1000 MeV/$c^2$ and 30 MeV/$c^2$ at 1500 MeV/$c^2$.

We present the mass spectra of the identified $K^+K^-$ and $p\bar{p}$ pairs in Fig.7. The $K^+K^-$ spectrum rises sharply at threshold to a level $\sim$7% of the $\pi^+\pi^-$ spectrum up to 1400 MeV/$c^2$. The distribution does not show the rapid fall between 1400 and 1600 MeV/$c^2$ observed in the $\pi^+\pi^-$ spectrum, with the result that at (1600 ± 50) MeV/$c^2$ the $K\bar{K}/\pi\pi$ ratio is (55 ± 11)%. More statistics are required to establish whether the $K^+K^-$ data exhibit an excess of events around $M_{K\bar{K}} \sim 1575$ MeV/$c^2$. It should be noted in this context that the upper limit on K identification in the drift chamber cuts increasingly into the spectrum above 1600 MeV/$c^2$. For completeness, the $p\bar{p}$ data, consisting of only 19 events, are shown in Fig.7b.

## V. <u>MASS SPECTRA AT $\sqrt{s}$= 45 GeV</u>

Data were taken at $\sqrt{s}$= 45 GeV in a special ISR run of only $\sim$ 2 days with a luminosity $\sim 1 \times 10^{31}$ cm$^{-2}$sec$^{-1}$. The experimental trigger was identical to that used for the data at higher energy, and the events have been analysed with precisely the same cuts. For fixed angular coverage of the forward telescopes the $|t|$ range decreases by a factor of $\sim (45/63)^2$ to $0.008 < |t| < 0.023$ (GeV/c)$^2$. The trigger rate decreased by a factor $\sim$ 0.4. The difference in t ranges between the two sets of data will give rise to a factor of $\sim$ 0.3 - 0.4, depending upon the slope, $\alpha$, in t.

The data at 45 GeV consist of 38,500 triggered events. As expected, $\sum p_y$ for the central hadron pair peaks at ± 0.23 GeV/c. After applying all the same cuts we obtain 2321 exclusive $h^+h^-$ events with $\sim$ 5% background ; 2293 events were identified as $\pi^+\pi^-$, 20 as $K^+K^-$ and none as $p\bar{p}$.
The $\pi^+\pi^-$ mass spectrum is shown in Fig. 8. The solid line is a hand-drawn curve through the $\sqrt{s}$ = 63 GeV data, normalised to the same number

of events. The distributions are clearly very similar, with precisely the same structures being observed up to masses ~ 1800 MeV/$c^2$.

## VI. ANGULAR DISTRIBUTIONS AT $\sqrt{s}$ = 63 GeV

In order to investigate further the nature of the $\pi^+\pi^-$ structures, we have examined the normalized moments of the angular distributions. For the purpose, we choose a coordinate system where, in the $\pi\pi$ rest frame, the z-axis is along the t-channel axis, $\vec{p}_1-\vec{p}_3$ or $\vec{p}_2-\vec{p}_4$, and the y-axis is along the direction $\vec{p}_1\times\vec{p}_3$ or $\vec{p}_2\times\vec{p}_4$ (on alternate events).(Choosing the y-axis to be perpendicular to the production plane in the pp c.m. system gives essentially identical results.) In this coordinate frame, the unnormalized moments are defined by [9]:

$$\langle D^L_{M0} \rangle = H(LM) = \frac{1}{N} \sum_{i=1}^{N} D^L_{M0}(\theta_i, \phi_i, 0)$$

where

$$D^{L*}_{M0}(\theta,\phi,0) = \sqrt{\frac{4\pi}{2L+1}}\; Y^L_M(\theta,\phi)$$

and the angles $(\theta,\phi)$ describe the $\pi^+$ direction in the $\pi^+\pi^-$ rest frame and N is the number of events in a given mass bin.

We find that the moments H(11), H(20), H(22), H(31) and H(40) show definite non-zero structures as a function of the mass, while all other moments up to L=M=4 exhibit no significant structures and are consistent with zero throughout the mass region. The moments, shown in Fig. 9, are uncorrected for acceptance and the curves show the Monte Carlo predictions, assuming s-wave decay of the di-pion system. The magnitudes of the H(20), H(22) and H(40) moments are clearly largely accounted for by the Monte Carlo calculation, and we conclude that it is the s-wave that dominates the $\pi\pi$ system below 1100 MeV/$c^2$, as expected.

However, the structure around 750 MeV/$c^2$ in H(11), also seen in H(31), is not caused by acceptance effects. Although a $\rho^0$ signal is not visible in the $\pi^+\pi^-$ mass spectrum, our data nevertheless contain a small amount of $\rho^0$, producing interference effects between the s- and p-waves. The presence of the $\rho^0$ in our data indicates a small but significant contribution from a process other than double pomeron exchange. Between the $\rho^0$ mass and 1100 MeV/$c^2$ we do not find any significant structure in the moments beyond that accounted for by the finite acceptance. In particular it seems clear that the sharp drop at 1 GeV/$c^2$ seen in the mass spectrum is confined to that of the s-wave, indicating clearly the influence of the S* (980).

There is an indication that some d-wave is present in our data, in the 1200-1400 MeV/$c^2$ region, possibly due in part to the f(1270). This region may also contain the $\epsilon$(1300), but final conclusions must await further analysis.

## VII. DISCUSSION

Our data demonstrate very clearly the process of exclusive central $\pi^+\pi^-$ production, with little contribution from reggeon exchange (apart from the pomeron) in contrast to experiments at lower energies. We obtain directly from the experiment a predominantly s-wave $\pi^+\pi^-$ spectrum, which contains much structure.

In the low mass region, according to Pumplin and Henyey [1] the pomeron-pomeron interaction is mediated by one-pion exchange with a strong final-state interaction giving rise to the observed s-wave behaviour. On the other hand, from duality one may also conclude that the same sub-process is mediated via s-channel resonances. The broad peak in the region around 500 MeV/$c^2$ may then be a manifestation of the strong s-wave $\pi\pi$ attraction previously referred to as the $\sigma$ or $\epsilon$(600). To the extent that the S*(980) is seen clearly in the DPE process, which has zero quark content in the initial state, the S*(980) may well harbour a large admixture of a $J^{PC}=0^{++}$ glueball. This has been suggested by several authors [10] and Novikov et al [11] (and others) conclude that there must be very strong mixing between $0^+$ $q\bar{q}$ and gg states.

Between 1000 and 1600 MeV/$c^2$ structures are observed in the $\pi^+\pi^-$ channel and possibly also in $K^+K^-$. The $D^2_{oo}$ and $D^4_{oo}$ moments in the $\pi^+\pi^-$ channel are suggestive of some d-wave contribution near 1300 MeV/$c^2$. These effects are consistent with the presence of f(1270), which could be responsible for the peak in the $\pi^+\pi^-$ mass plot, although the $0^+$ $\varepsilon$(1300) is another known state in this region. This effect is followed by a sharp drop in di-pion production near 1500 MeV/$c^2$ ; a striking feature for which we have no explanation. The $K^+K^-$ spectrum may also exhibit structure in the same region. This could indicate the presence of the f'(1515) or at the same time be a signal for a gluonium state [12].

The existence of the rather flat plateau in the $\pi^+\pi^-$ mass spectrum from 1600-2300 MeV/$c^2$, followed by a relatively rapid decrease (see Fig.4c), is an observation that we have not understood in terms of known states. More statistics may be required to shed light on the dynamical origin of this region of the mass spectrum, and other channels eg $\pi\pi\pi\pi$, $KK\pi\pi$ may provide clues. A possible hypothesis is that a heavy state eg $\varepsilon$(2300), $0^+4^{++}$, plays a similar role to that of the S*(980) in causing a rapid drop in the cross section. Clearly the 3 GeV/$c^2$ region, where the $c\bar{c}$ threshold occurs, would also be of great interest to study with higher statistics.

ACKNOWLEDGEMENTS

Support from the Research Councils in our home countries is gratefully acknowledged. We would like to thank in particular the workshops of the Cavendish Laboratory, Cambridge, the Physics Dept, Queen Mary College, the Physics Apparatus Group at the Rutherford Appleton Laboratory and the Experimental Support Group of the ISR at CERN for technical assistance.

REFERENCES

[1] R. Schankar, Nucl. Phys. B63 (1974) 168
D.M. Chew and G.F. Chew, Phys. Lett 53B (1974) 191
D.M. Chew, Phys. Lett. 65B (1976) 367
J. Pumplin and F.S. Henyey, Nucl. Phys. B117 (1976) 377
B.R. Desai, B.C. Chen and M. Jacob, Nucl. Phys. B142 (1978) 258

[2] See. e.g.
H. Fritzch and M. Gell Mann, Proc. XVI Int. Conf. on HEP, Chicago (1972) p. 135
H. Fritzch and P. Minkowski, Nuovo Cimento 30A (1975) 393
R.L. Jaffe, K. Johnson, Phys. Lett. 60B (1976) 201
C.E. Carlson, J.J. Coyne, P.M. Fishbane, F. Gross and S. Meshkov, Phys. Lett. 99B (1981) 353
J.F. Donoghue, K. Johnson and B.A. Li, Phys. Lett. 99B (1981) 416
H.J. Lipkin, Phys. Lett. 106B (1981) 114
I. Cohen, N. Isgur and H.J. Lipkin, Phys. Lett. 48 (1982) 1074

[3] F.E. Low, Phys. Rev. D12 (1975) 163
S. Nussinov, Phys. Rev. Lett. 34 (1975) 1286
S. Nussinov, Phys. Rev. D14 (1976) 246
A. Donnachie and P.V. Landshoff, Phys. Lett. 123B (1983) 345
A. Donnachie and P.V. Ladshoff, DAMTP Preprint 82/33 (1983)

[4] D. Robson, Nucl. Phys. B130. (1977) 328

[5] M. Derrick et al., Phys. Rev. D9 (1974) 1215
J.C.M. Armitage et al., Phys. Lett. 82B (1975) 149
M. Della Negra et al., Phys. Lett. 65B (1976) 394
V. Blobel et al., Nucl. Phys. B69 (1974) 237
D. Denegri et al., Nucl. Phys. B98 (1975) 189

[6] L. Baksay et al., Phys. Lett. 61B (1976) 89
H. de Kerret et al., Phys. Lett. 68B (1977) 385
D. Drijard et al., Nucl. Phys. B143 (1978) 61
R. Waldi, K.R. Schubert and K. Winter, Heidelberg Preprint IHEP-HD/83-2, submitted to Z. Phys.

[7] H. Gordon et al., Nucl. Instrum. Methods 196 (1982) 303
O. Botner et al., Nucl. Instrum. Methods 196 (1982) 315

[8] M.G. Albrow et al., Rutherford Preprint RL-83-014, to be published in Nucl. Instrum. Methods

[9] S.U. Chung, CERN Yellow Report 71-8

[10] Y.M. Cho, J.L. Cortes and X.Y. Pham, PAR-LPTHE 81-08 (1981)
Y.M. Cho and W. Weinzierl, PAR-LPTHE 81-10 (1981)
E. Etkins et al., Phys. Rev. D25 (1982) 2446
S. Minami, Osaka City Univ. preprint OCV-103 (1983)

[11] V.A. Novikov, M.A. Shifman, A.I. Vainshtein and V.I. Zakharov, Nucl. Phys. B191 (1981) 301

[12] J. Rosner, Phys. Rev. D24 (1981) 1347
N.A. Törnqvist, Helsinki, preprint HU-TFT 83-23 (1983)

FIGURE CAPTIONS

Fig. 1 Schematic side view of the apparatus. Only the right-hand forward detectors are shown ; the apparatus is left-right symmetric.

Fig. 2 (a) Distribution of $\Sigma p_y$ (vertical momentum) for the central particles, separately for the UP.UP and DOWN.DOWN trigger configuration, after selecting events with 2 central tracks. The shaded histogram shows the combined contribution from ++ and -- charge-pairs

(b) Difference between $\Sigma p_x$ of the initial pp state and the final $pph^+h^-$ state, after requiring $\Sigma p_y = 0 \pm 60$ MeV/c. Note the logarithmic scale. An estimate of the background is shown by the dashed curve.

Fig. 3 (a) Distribution of Feynman $x_F$, uncorrected for acceptance, of the final state protons for the $\pi^+\pi^-$ sample, as inferred from $E, p_z$ constraints.

(b) Observed distribution of rapidity y of the pions in the final $\pi^+\pi^-$ sample (histogram) and of the $(\pi^+\pi^-)$ system (circles).

Fig. 4 (a) Mass spectrum, not corrected for acceptance, of the central $\pi^+\pi^-$ events in 25 MeV/$c^2$ bins.
(b) shows the region 1000-2300 MeV/$c^2$ with an expanded vertical scale.
(c) shows the region 1500-3500 MeV/$c^2$ in 50 MeV/$c^2$ bins.

Fig. 5 Mass spectrum of the central $\pi^+\pi^-$ events with a logarithmic ordinate. The data are not corrected for acceptance.

Fig. 6 The relative acceptance (arbitrary scale with maximum value unity) as a function of $M(\pi^+\pi^-)$ calculated from Monte Carlo events generated within a DPE model with s-wave decay of the di-pion system.

Fig. 7 (a) Uncorrected mass spectrum of the exclusive $pp \to ppK^+K^-$ events. Loss of kaon identification artificially cuts off the spectrum above ~1600 MeV/$c^2$.

(b) Mass spectrum of the exclusive $pp \to ppp\bar{p}$ events.

Fig. 8 Mass spectrum, as for fig.5, but for $\sqrt{s}$= 45 GeV. The solid line is hand-drawn through the data points of fig.5 ($\sqrt{s}$= 63 GeV), normalised to the same total number of events.

Fig. 9 The normalised moments a) $\langle Re\, D^1_{10} \rangle$, b) $\langle D^4_{00} \rangle$, c) $\langle D^2_{00} \rangle$, d) $\langle Re\, D^2_{20} \rangle$ versus mass of the $\pi^+\pi^-$ system. The solid curves are Monte Carlo results for the effective moments produced by the acceptance of the apparatus for s-wave decay of the $\pi^+\pi^-$ system.

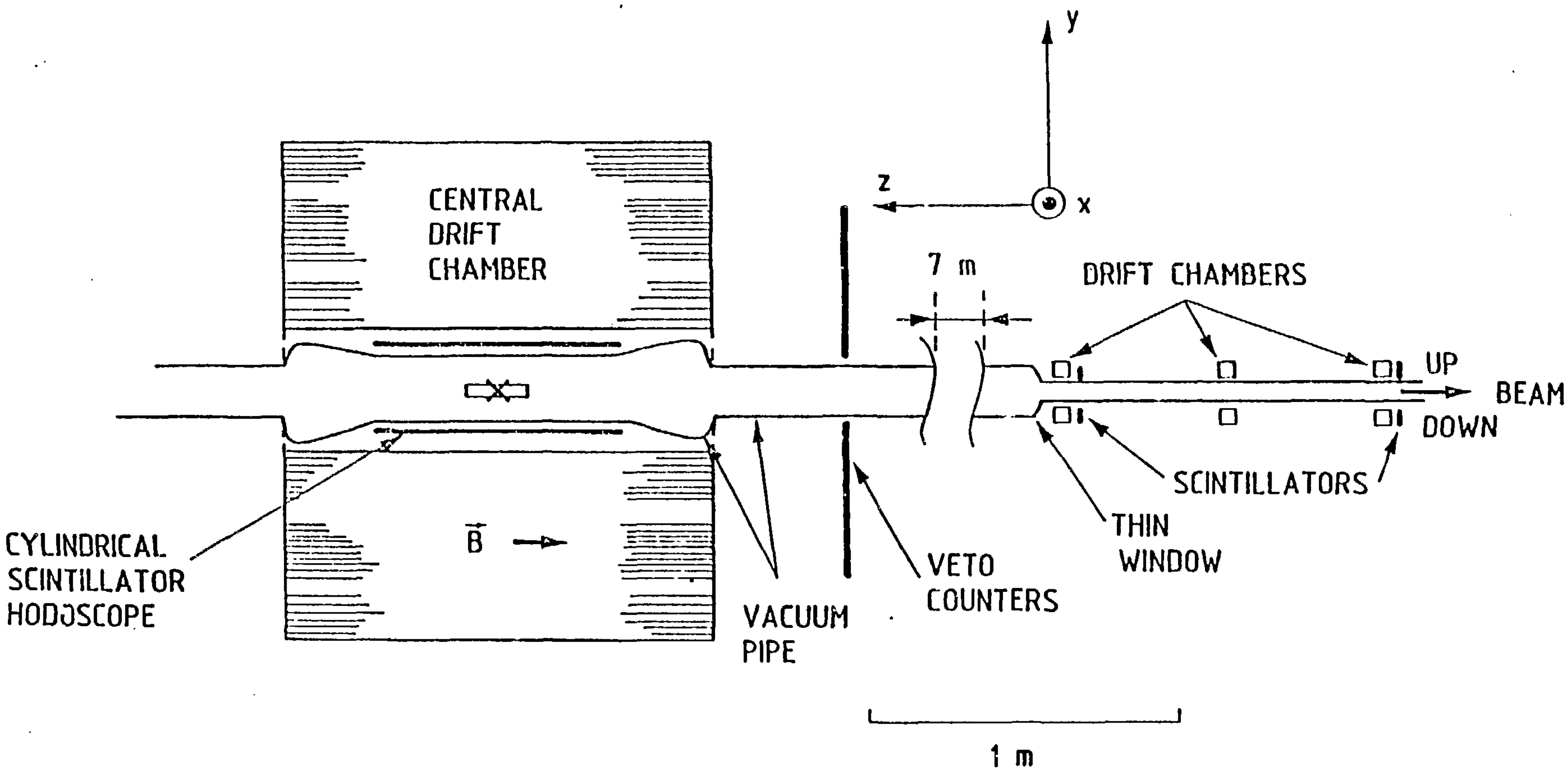

y
z
x
CENTRAL
DRIFT
CHAMBER
7 m
DRIFT CHAMBERS
UP
BEAM
DOWN
SCINTILLATORS
THIN
WINDOW
VETO
COUNTERS
VACUUM
PIPE
CYLINDRICAL
SCINTILLATOR
HODOSCOPE
B
1 m


Fig. 1

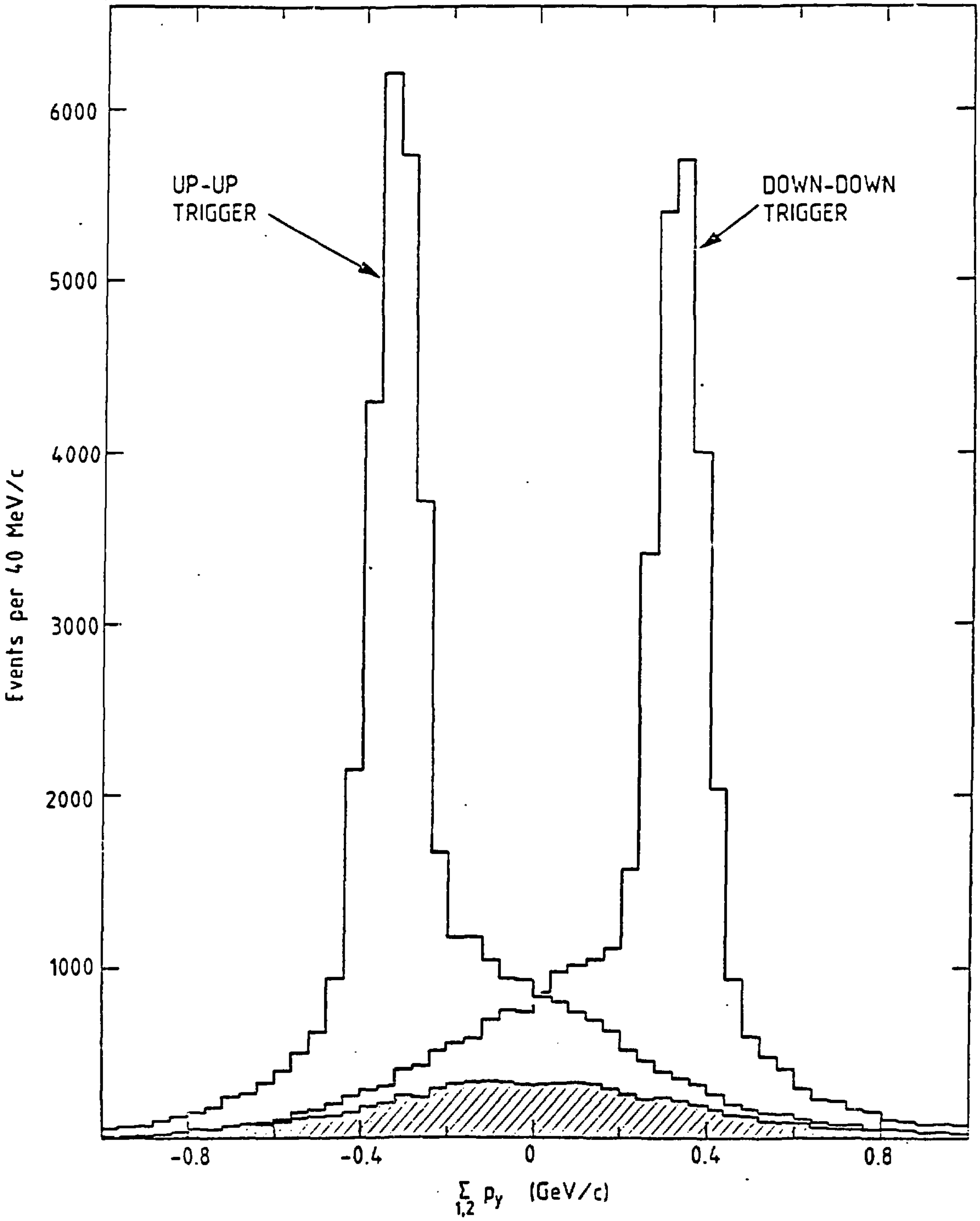
UP-UP
TRIGGER
DOWN-DOWN
TRIGGER
6000
5000
4000
3000
2000
1000
Events per 40 MeV/c
-0.8
-0.4
0
0.4
0.8
$\sum_{1,2} p_y$ (GeV/c)

Fig. 2a

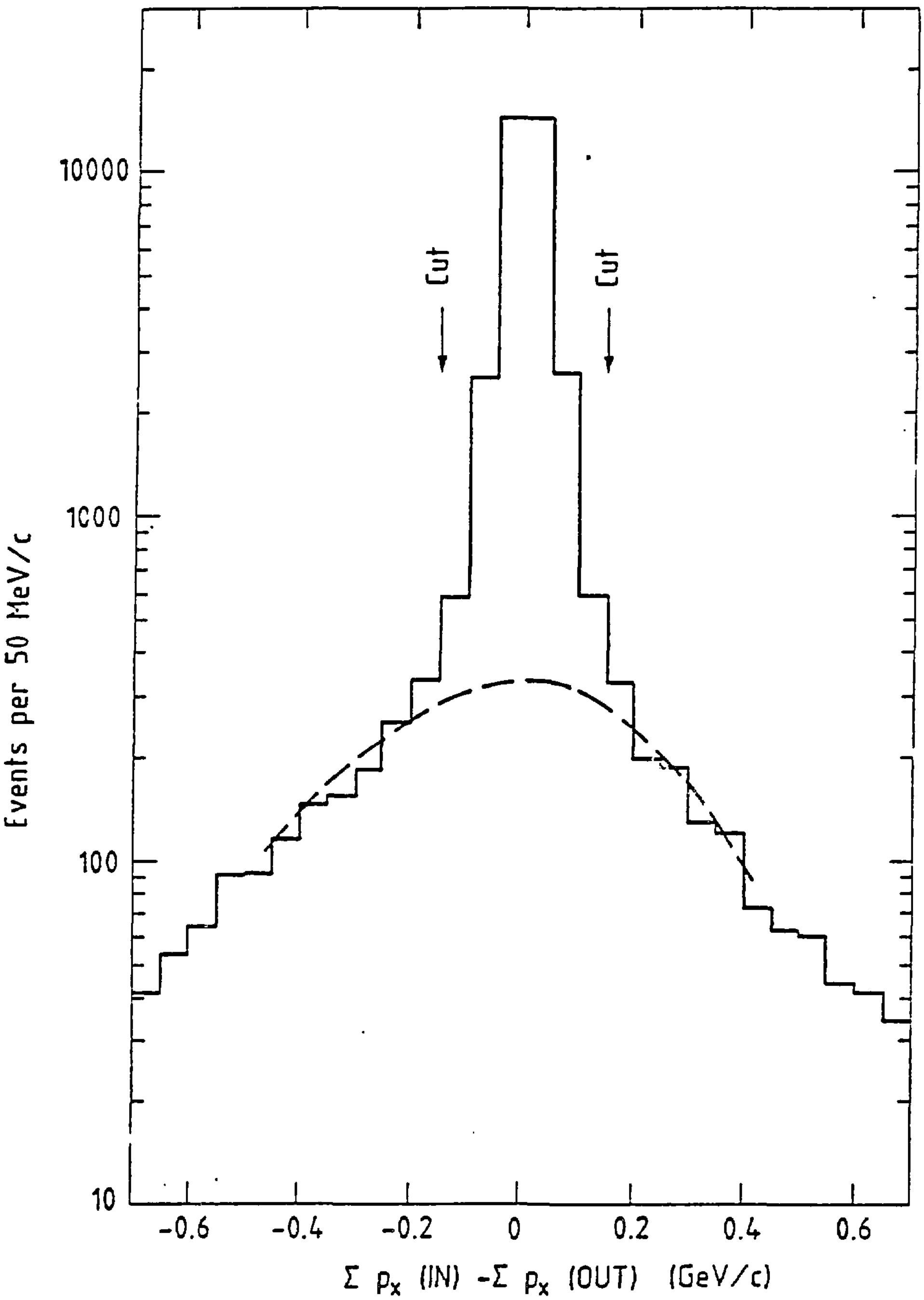
10000
1000
100
10
Events per 50 MeV/c
Cut
Cut
-0.6
-0.4
-0.2
0
0.2
0.4
0.6
Σ p_x (IN) -Σ p_x (OUT) (GeV/c)

Fig. 2b

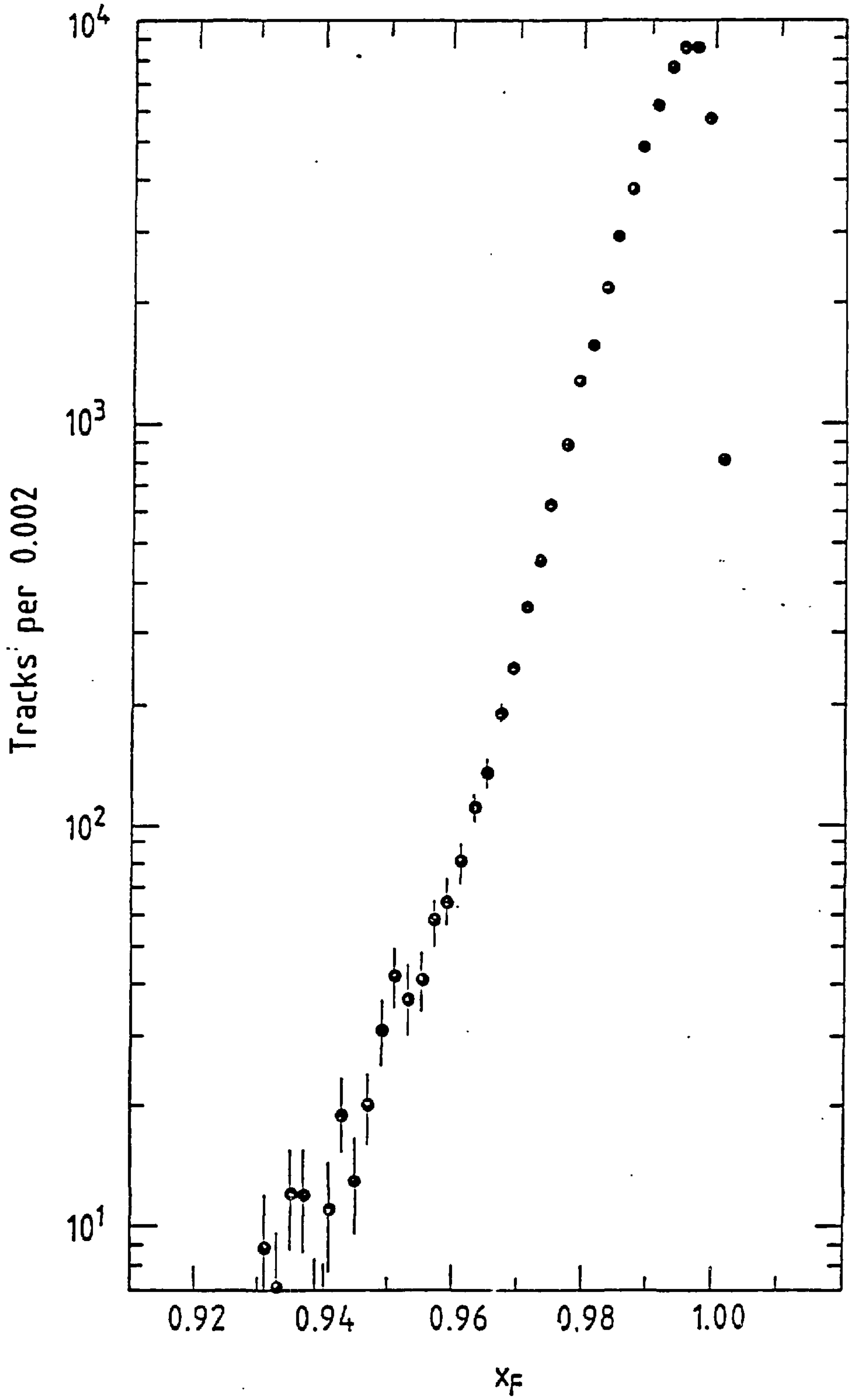


Fig. 3a

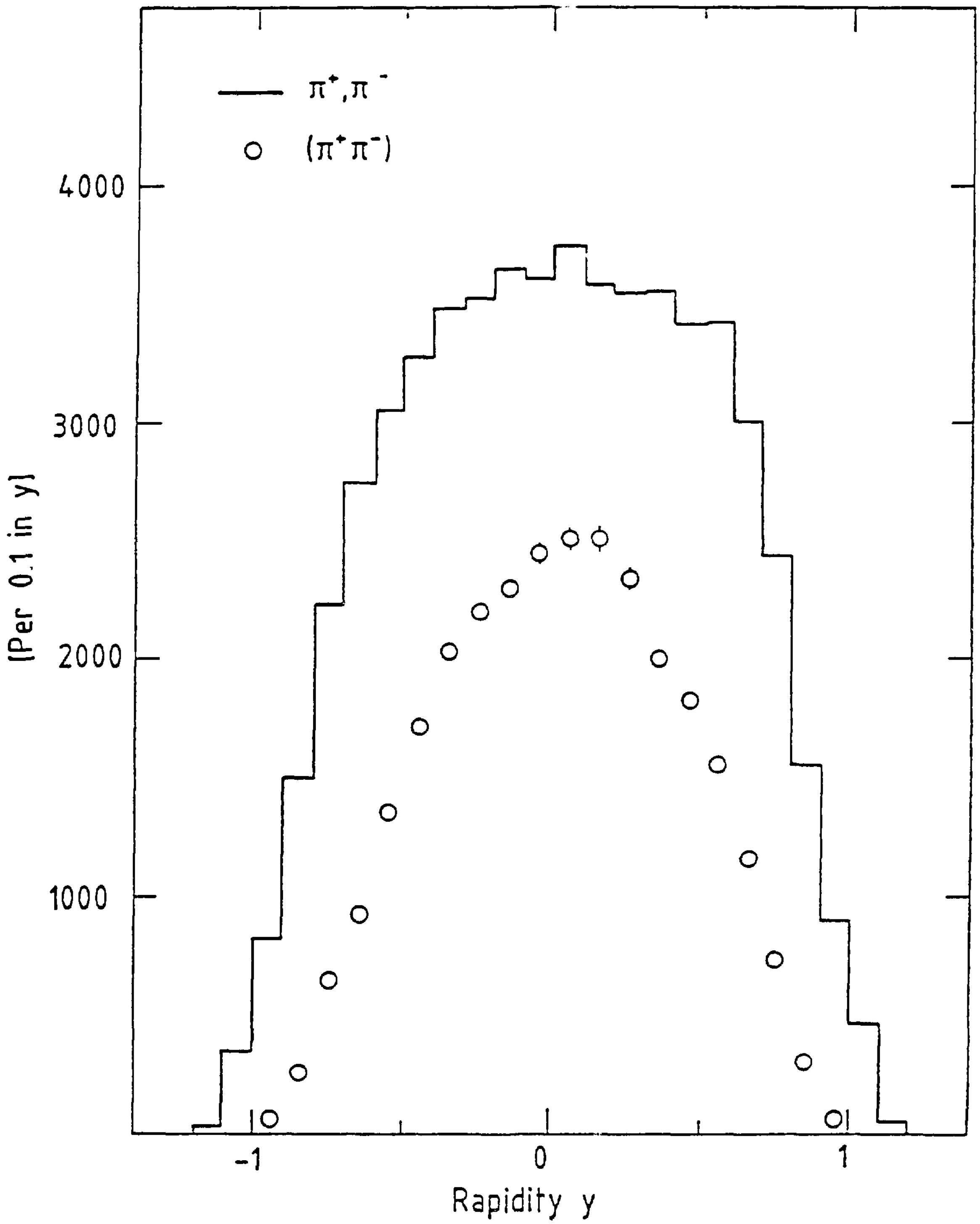


Fig. 3b

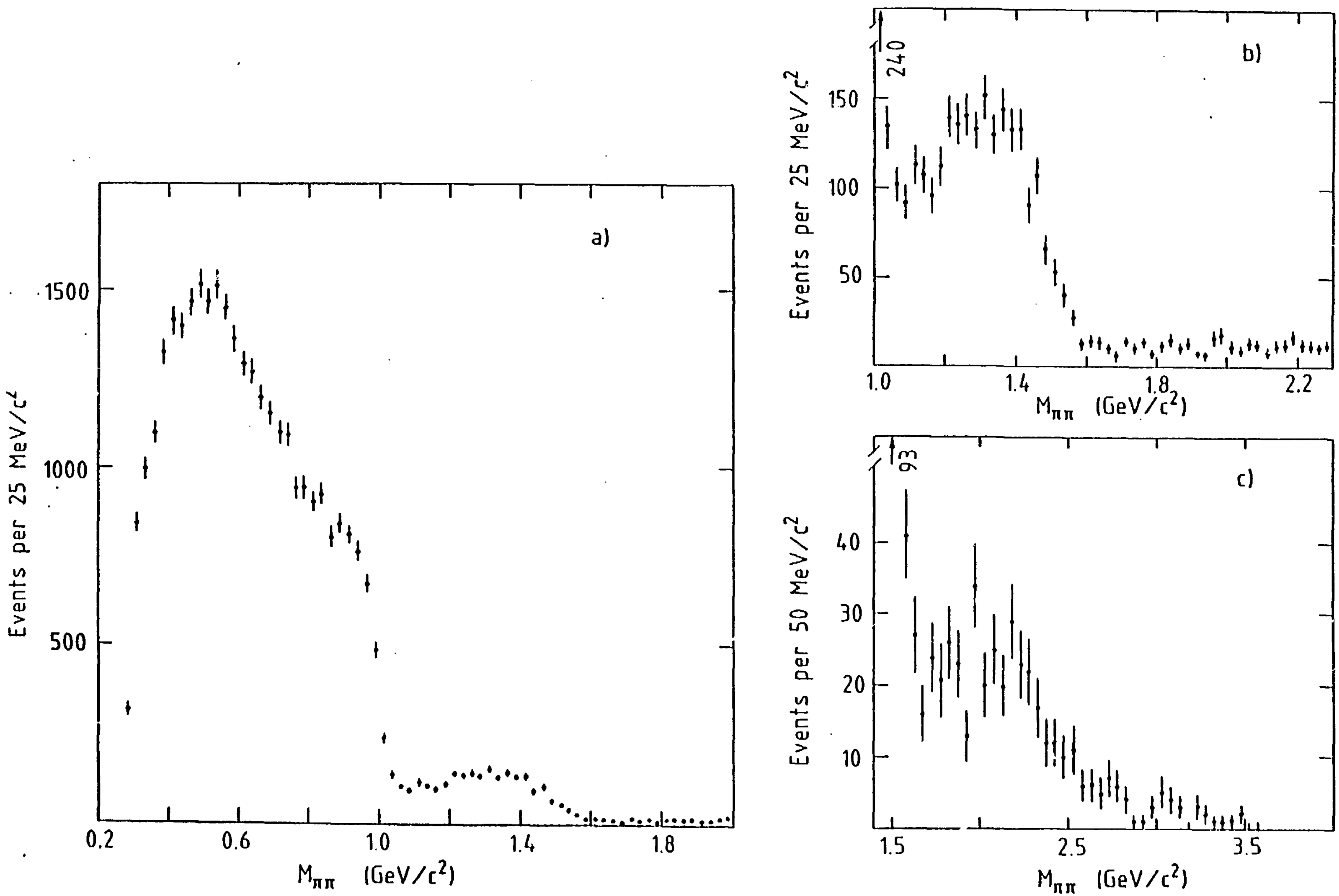
a)
Events per 25 MeV/c²
1500
1000
500
0.2
0.6
1.0
1.4
1.8
$M_{\pi\pi}$ (GeV/c²)
b)
240
Events per 25 MeV/c²
150
100
50
1.0
1.4
1.8
2.2
$M_{\pi\pi}$ (GeV/c²)
c)
93
Events per 50 MeV/c²
40
30
20
10
1.5
2.5
3.5
$M_{\pi\pi}$ (GeV/c²)

Fig. 4

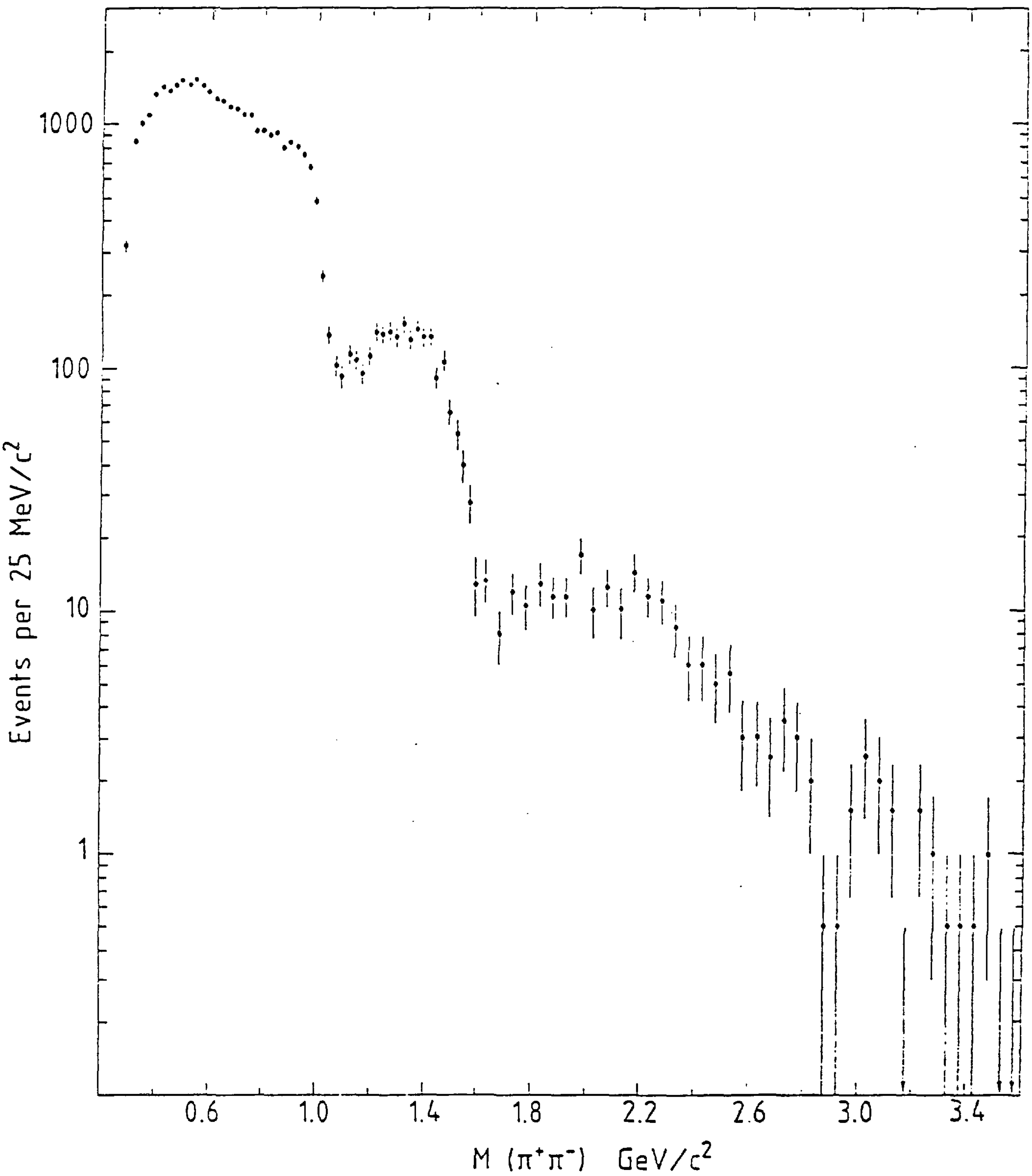

1000
100
10
1
Events per 25 MeV/c²
0.6
1.0
1.4
1.8
2.2
2.6
3.0
3.4
M (π⁺π⁻) GeV/c²


Fig. 5

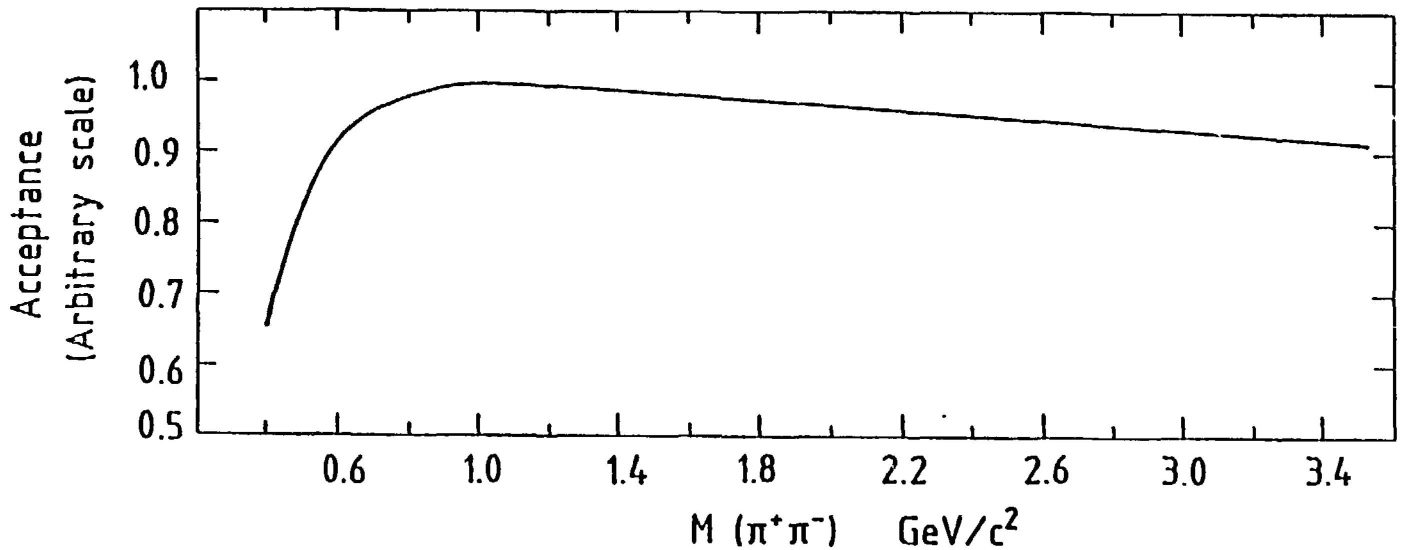
Acceptance
(Arbitrary scale)
1.0
0.9
0.8
0.7
0.6
0.5
0.6
1.0
1.4
1.8
2.2
2.6
3.0
3.4
M (π⁺π⁻) GeV/c²

Fig. 6

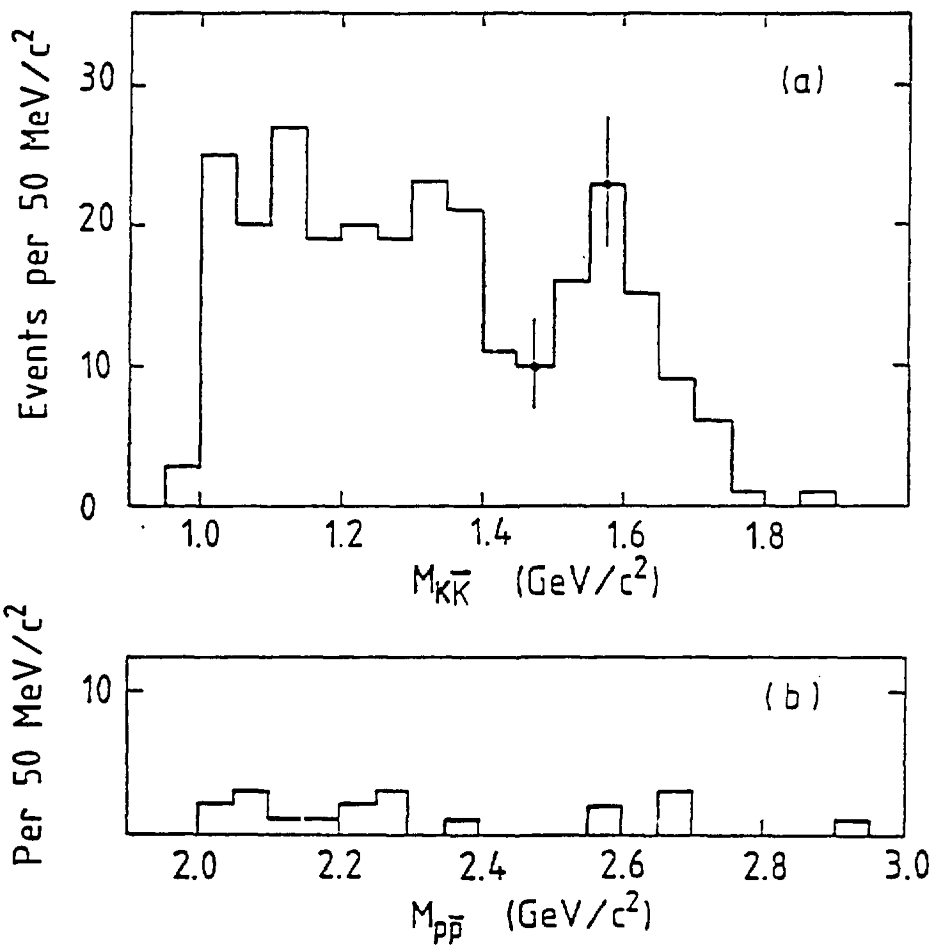
(a)
Events per 50 MeV/c²
30
20
10
0
1.0
1.2
1.4
1.6
1.8
M_KK̄ (GeV/c²)
(b)
Per 50 MeV/c²
10
2.0
2.2
2.4
2.6
2.8
3.0
M_pp̄ (GeV/c²)

Fig. 7

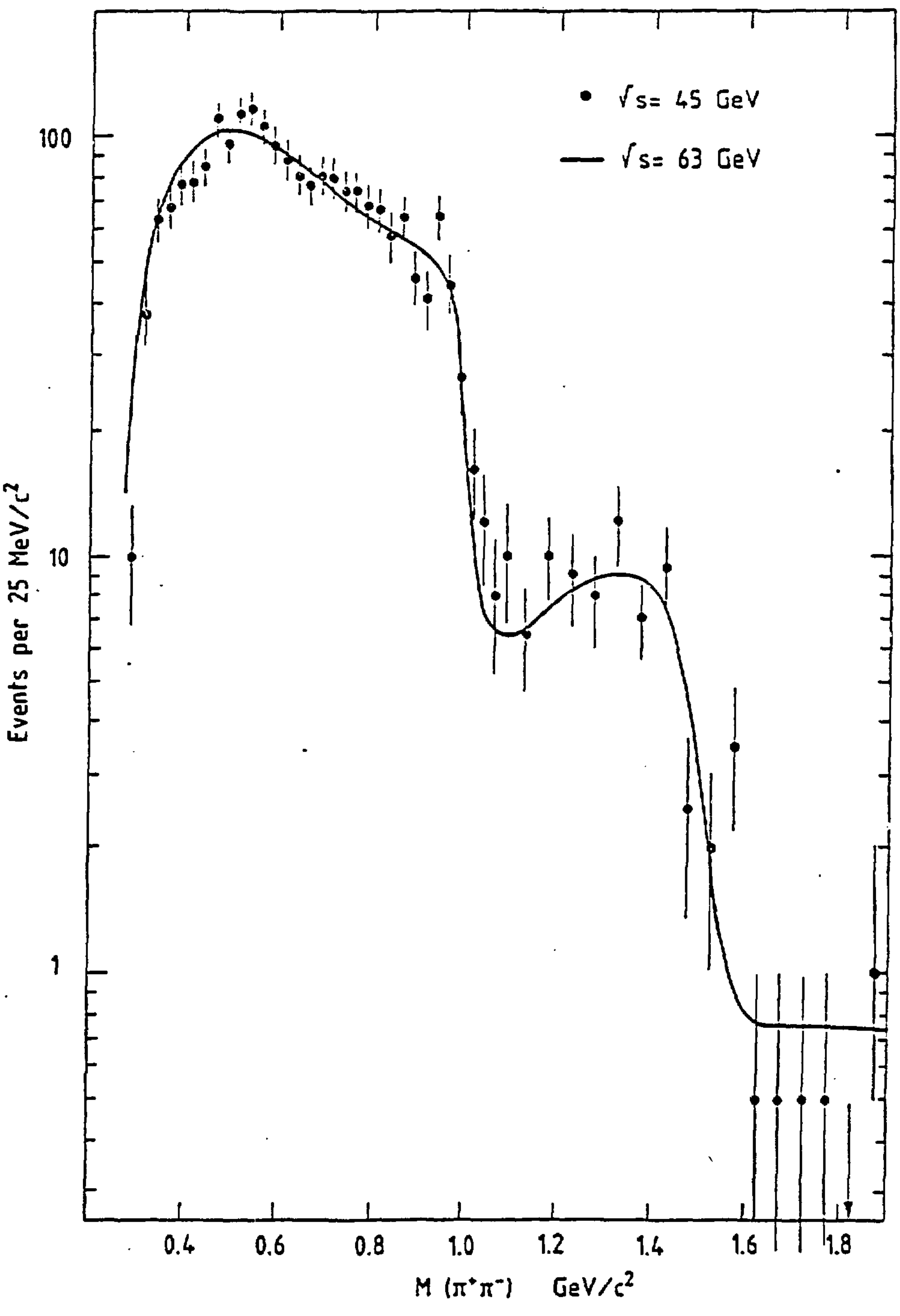

√s= 45 GeV
√s= 63 GeV
100
10
1
Events per 25 MeV/c²
0.4
0.6
0.8
1.0
1.2
1.4
1.6
1.8
M (π⁺π⁻) GeV/c²


Fig. 8

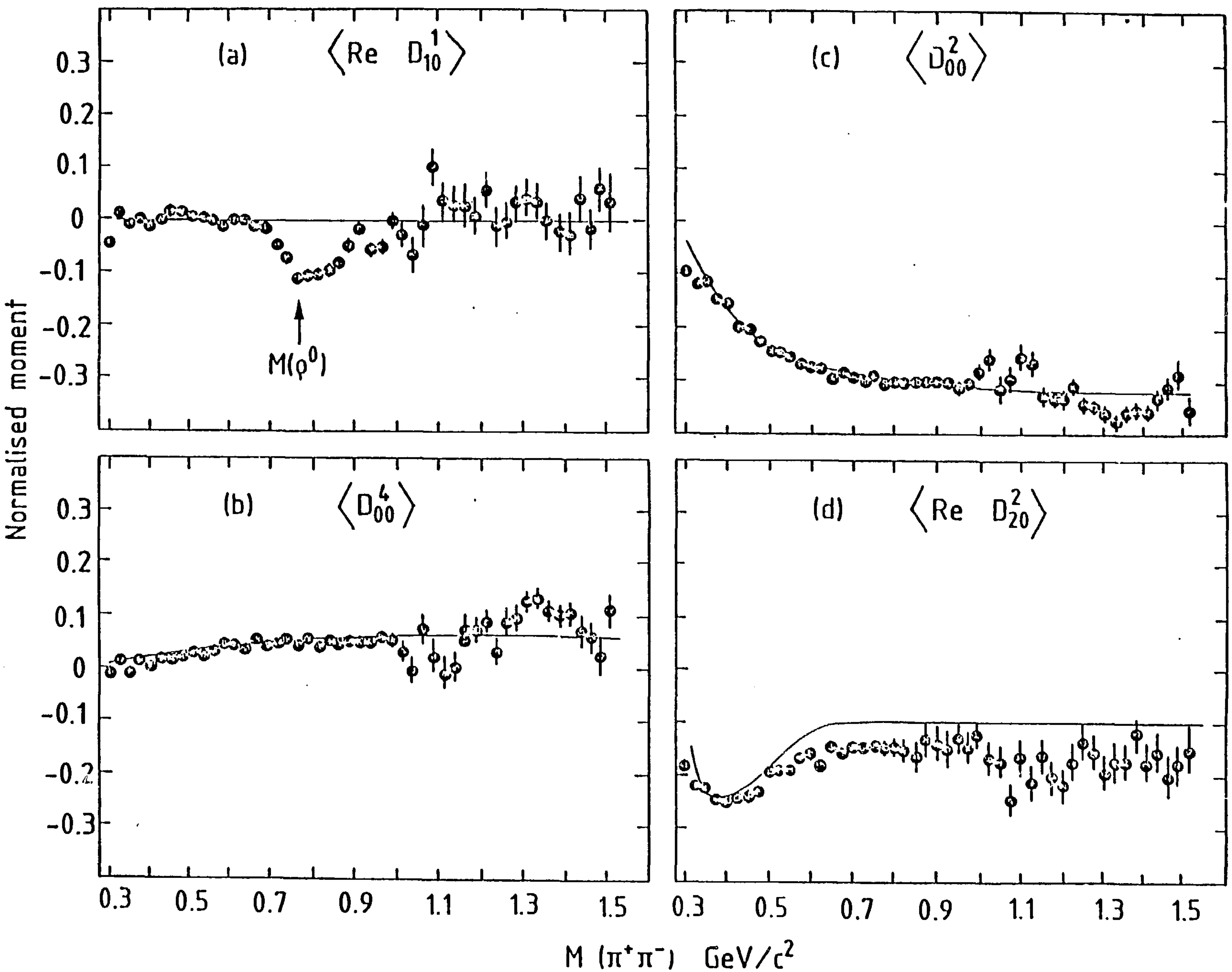
(a)
$\langle Re\ D^1_{10} \rangle$
$M(\rho^0)$
(b)
$\langle D^4_{00} \rangle$
(c)
$\langle D^2_{00} \rangle$
(d)
$\langle Re\ D^2_{20} \rangle$
Normalised moment
0.3
0.2
0.1
0
-0.1
-0.2
-0.3
0.3
0.5
0.7
0.9
1.1
1.3
1.5
$M\ (\pi^+\pi^-)\ GeV/c^2$

Fig. 9